

Van der Waals interaction between two crossed carbon nanotubes

Alexander I. Zhbanov, Evgeny G. Pogorelov,* and Yia-Chung Chang
*Research Center for Applied Sciences, Academia Sinica, 128,
Section 2, Academia Road Nankang, Taipei 115, Taiwan.*
(Dated: May 26, 2022)

The analytical expressions for the van der Waals potential energy and force between two crossed carbon nanotubes are presented. The Lennard-Jones potential for two carbon atoms and the method of the smeared out approximation suggested by L.A. Girifalco were used. The exact formula is expressed in terms of rational and elliptical functions. The potential and force for carbon nanotubes were calculated. The uniform potential curves for single- and multi- wall nanotubes were plotted. The equilibrium distance, maximal attractive force, and potential energy have been estimated.

PACS numbers: 7970+g, 8105Tp

I. INTRODUCTION

The van der Waals (VDW) interaction plays very important role in Nano Electro Mechanical systems and Nano Electronic Devices^{1,2}. Carbon nanotubes (CNTs) are promising material for creation a nanotweezers^{3,4}, nanoswitches^{5,6,7}, bearings^{8,9,10}, nanotube random access memory^{11,12}, etc. The VDW forces are very critical for understanding the growth mechanism of fullerenes and nanotubes^{13,14,15} and formation process of ropes and bundles^{16,17,18}. Potentials for graphite layers^{19,20}, two fullerenes^{21,22,23,24}, fullerene and surface^{25,26}, nanotube and surface^{9,27,28}, fullerenes inside and outside of nanotubes^{29,30,31,32,33} are well studied. There are a number of publications devoted to interaction between the inner and the outer parallel tubes such as single- (SWNTs)^{29,34,35,36}, double^{37,38}, and multi-wall nanotubes (MWNTs)^{39,40,41}.

The present work is dedicated to interplay between two CNTs crossed at arbitrary angle. Problems related with application of molecular dynamics and density functional theory for such kind of calculations are discussed for example in Refs. 29 and 36.

To evaluate potential between two crossed SWNTs or MWNTs we apply the continuum Lenard-Jones (LJ) model suggested by L.A. Girifalco²¹.

The model potentials for the VDW interaction are based on empirical functions whose parameters are obtained from experiment. It is remarkable that they have been so successful in providing a unified, consistent description of the properties that depend on the weak interactions between and among graphene sheets, fullerene molecules, and nanotubes.

II. ANALYTICAL APPROACH

A. Model

The LJ potential for two carbon atoms in graphene-graphene structure is

$$\varphi(r) = -\frac{A}{r^6} + \frac{B}{r^{12}}. \quad (1)$$

where r is a distance, $A = 15.2 \text{ eV} \cdot \text{\AA}^6$ and $B = 24100 \text{ eV} \cdot \text{\AA}^{12}$ are the attractive and repulsive constants respectively²⁹. We approximate the potential between two crossed SWNTs by integration of LJ potential

$$\varphi_{tt} = \nu^2 \int \varphi(r) d\Sigma_1 d\Sigma_2. \quad (2)$$

Mean surface density of carbon atoms for hexagonal structure is

$$\nu = \frac{4}{3\sqrt{3}a_1^2} \approx 0.393 \text{ atom per } \text{\AA}^2, \quad (3)$$

where $a_1 = 1.42 \text{\AA}$ is observed value of the C-C bond lengths for periodic graphite³⁷. If we know van der Waals interaction between two SWNTs then we may obtain interaction between MWNTs by summation over all pairs of layers⁴⁰.

B. Ancillary integrals

To calculate the VDW interaction between two nanotubes we have to take few useful integrals. For integral of LJ potential between two straight lines

$$I_{ll}(r) = \int \varphi(r) dl_1 dl_2, \quad (4)$$

we obtain

$$I_{ll}(r) = \frac{\pi}{\sin \gamma} \left(-\frac{A}{2r^4} + \frac{B}{5r^{10}} \right), \quad (5)$$

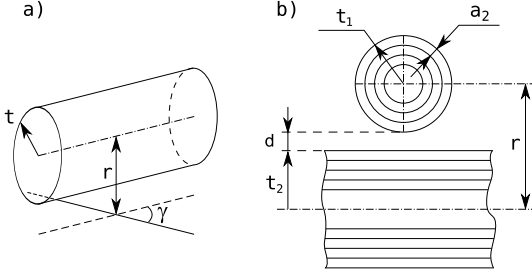


FIG. 1: Schematic drawing of interaction between: a) SWNT and line; b) two MWNTs

where γ is angle, r is distance between lines, and index ll means “line-line”. For next integral between line and tube we have

$$I_{lt}(r, t) = t \int_{-\pi}^{\pi} I_{ll}(r - t \sin \beta) d\beta, \quad r > t, \quad (6)$$

where t is tube radius, r is distance between line and axis of tube, and index lt means “line-tube”. Figure 1a illustrates the schematic image of SWNT and line. Introducing new variable $u = \tan(\beta/2)$ and using method of partial fractions we get

$$\begin{aligned} I_{lt}(r, t) &= \frac{1}{\sin \gamma} \left(-\frac{A \cdot \varkappa^3 G_A(\varkappa)}{2r^3} + \frac{B \cdot \varkappa^9 G_B(\varkappa)}{5r^9} \right) \\ &= \frac{1}{\sin \gamma} \left(-\frac{A \cdot G_A(\varkappa)}{2t^3} + \frac{B \cdot G_B(\varkappa)}{5t^9} \right), \end{aligned} \quad (7)$$

where

$$\begin{aligned} \varkappa &\equiv \frac{r}{t}, \quad G_A(\varkappa) = \frac{\pi^2 \varkappa (2\varkappa^2 + 3)}{(\varkappa^2 - 1)^{\frac{7}{2}}}, \\ G_B(\varkappa) &= \frac{\pi^2 \varkappa (128\varkappa^8 + 2304\varkappa^6 + 6048\varkappa^4 + 3360\varkappa^2 + 315)}{64(\varkappa^2 - 1)^{\frac{19}{2}}}. \end{aligned}$$

C. Tube-tube interaction potential

Figure 1b schematically shows the interaction between two MWNTs crossed at right angle. Parameter $a_2 = 3.44\text{\AA}$ is the average distance between two layers in MWNTs³⁷, d is the gap between tubes.

In particular case these tubes may consist only of one layer. We notice t_1 as a radius of first SWNT, and t_2 as a radius of second one ($r = d + t_1 + t_2$). The interaction potential between two SWNTs is

$$\varphi_{tt}(r, t_1, t_2) = 2\nu^2 \int_{r-t_2}^{r+t_2} I_{tt}(x, t_1) \sqrt{1 + y^2(x)} dx, \quad (8)$$

where $y(x) = \sqrt{t_2^2 - (x-r)^2}$, index tt means “tube-tube”.

Introducing dimensionless parameters

$$\varkappa = \frac{x}{t_1}, \quad b_1 = \frac{r}{t_1}, \quad b_2 = \frac{r}{t_2}, \quad k = \frac{t_2}{t_1}, \quad (9)$$

and using (7) we have

$$\varphi_{tt}(r, t_1, t_2) = \nu^2 t_1 \int_{b_1-k}^{b_1+k} \frac{2k I_{tt}(\varkappa, t_1)}{\sqrt{k^2 - (\varkappa - b_1)^2}} d\varkappa. \quad (10)$$

After some transformations we write

$$\varphi_{tt}(r, t_1, t_2) = \frac{\nu^2}{\sin \gamma} \left(-\frac{A \cdot g_A}{r^2} + \frac{B \cdot g_B}{r^8} \right), \quad (11)$$

where multipliers for attractive and repulsive terms are

$$g_A(b_1, b_2) = \frac{b_1^2}{2} \int_{b_1-k}^{b_1+k} \frac{2k G_A(\varkappa)}{\sqrt{k^2 - (\varkappa - b_1)^2}} d\varkappa, \quad (12)$$

$$g_B(b_1, b_2) = \frac{b_1^8}{5} \int_{b_1-k}^{b_1+k} \frac{2k G_B(\varkappa)}{\sqrt{k^2 - (\varkappa - b_1)^2}} d\varkappa. \quad (13)$$

The obtained Eqs. (12, 13) represents the elliptic integrals. In modern mathematics elliptic integral is defined as integral $\int R(x, y) dx$, where $R(x, y)$ is rational function of x and y , and y^2 is a cubic or quartic polynomial in x . With the appropriate reduction formula every elliptical integral can be expressed in terms of elementary functions and canonical elliptic integrals of first, second and third kind. The method of integration is quite complicated but well known^{42,43,44,45}. We would like to present only final answer. For attractive part we have the dimensionless parameter

$$g_A = g_{AK} K(h) + g_{AE} E(h), \quad (14)$$

where

$$h = \frac{2\sqrt{b_1 b_2}}{\sqrt{(b_1 b_2 + b_1 - b_2)(b_1 b_2 + b_2 - b_1)}}, \quad (15)$$

$$\begin{aligned} g_{AK} &= - \left[2\pi^2 b_1^4 b_2^4 \sum_{i,j=1..3} \{p_{AK}\}_{ij} b_1^{2(i-1)} b_2^{2(j-1)} \right] \\ & \left[3(b_1 b_2 + b_1 + b_2)^2 (b_1 b_2 - b_1 - b_2)^2 (b_1 b_2 + b_1 - b_2)^{\frac{5}{2}} \right. \\ & \quad \left. \times (b_1 b_2 + b_2 - b_1)^{\frac{5}{2}} \right], \end{aligned} \quad (16)$$

$$\begin{aligned} g_{AE} &= \left[2\pi^2 b_1^4 b_2^4 \sum_{i,j=1..4} \{p_{AE}\}_{ij} b_1^{2(i-1)} b_2^{2(j-1)} \right] \\ & \left[3(b_1 b_2 + b_1 + b_2)^3 (b_1 b_2 - b_1 - b_2)^3 (b_1 b_2 + b_1 - b_2)^{\frac{5}{2}} \right. \\ & \quad \left. \times (b_1 b_2 + b_2 - b_1)^{\frac{5}{2}} \right], \end{aligned} \quad (17)$$

and matrixes of integer coefficients are

$$\{p_{AK}\} = \begin{bmatrix} 0 & 0 & -3 \\ 0 & 6 & -2 \\ -3 & -2 & 5 \end{bmatrix},$$

$$\{p_{AE}\} = \begin{bmatrix} 0 & 0 & 0 & 12 \\ 0 & 0 & -12 & -13 \\ 0 & -12 & 58 & -10 \\ 12 & -13 & -10 & 11 \end{bmatrix}.$$

Analogically for repulsive part we write the dimensionless parameter

$$g_B = g_{BK}K(h) + g_{BE}E(h), \quad (18)$$

where

$$g_{BK} = - \left[\pi^2 b_1^{10} b_2^{10} \sum_{i,j=1..12} \{p_{BK}\}_{ij} b_1^{2(i-1)} b_2^{2(j-1)} \right] / \left[6300(b_1 b_2 + b_1 + b_2)^8 (b_1 b_2 - b_1 - b_2)^8 \times (b_1 b_2 + b_1 - b_2)^{\frac{17}{2}} (b_1 b_2 + b_2 - b_1)^{\frac{17}{2}} \right], \quad (19)$$

$$g_{BE} = \left[\pi^2 b_1^{10} b_2^{10} \sum_{i,j=1..13} \{p_{BE}\}_{ij} b_1^{2(i-1)} b_2^{2(j-1)} \right] / \left[25200(b_1 b_2 + b_1 + b_2)^9 (b_1 b_2 - b_1 - b_2)^9 \times (b_1 b_2 + b_1 - b_2)^{\frac{17}{2}} (b_1 b_2 + b_2 - b_1)^{\frac{17}{2}} \right]. \quad (20)$$

Matrixes of integer coefficients $\{p_{BK}\}$ and $\{p_{BE}\}$ are placed in Table I and II respectively.

As we see the final result (11) is quite huge but it is working much better then usual numerical integration, because this analytical formula provides high accuracy and high speed of calculations.

D. Tube-tube force

The VDW resulting force caused by VDW interaction energy is

$$F(r) = - \frac{d\varphi_{tt}(r)}{dr}. \quad (21)$$

Using expressions⁴³

$$\frac{dK(x)}{dx} = \frac{E(x)}{(1-x^2)x} - \frac{K(x)}{x} \quad (22)$$

and

$$\frac{dE(x)}{dx} = \frac{1}{x}(E(x) - K(x)), \quad (23)$$

it is possible to obtain the analytical formula for VDW force. After usual differentiation over r we have

$$F(r, t_1, t_2) = \frac{\nu^2}{\sin \gamma} \left(- \frac{A \cdot f_A}{r^3} + \frac{B \cdot f_B}{r^9} \right), \quad (24)$$

where

$$f_A = f_{AK}K(h) + f_{AE}E(h), \quad (25)$$

$$f_B = f_{BK}K(h) + f_{BE}E(h). \quad (26)$$

The dimensionless coefficients for attractive and repulsive part of force are expressed as

$$f_{AK} = \left[2\pi^2 b_1^4 b_2^4 \sum_{i,j=1..5} \{q_{AK}\}_{ij} b_1^{2(i-1)} b_2^{2(j-1)} \right] / \left[3(b_1 b_2 + b_1 + b_2)^3 (b_1 b_2 - b_1 - b_2)^3 (b_1 b_2 + b_1 - b_2)^{\frac{7}{2}} \times (b_1 b_2 + b_2 - b_1)^{\frac{7}{2}} \right], \quad (27)$$

$$f_{AE} = - \left[4\pi^2 b_1^4 b_2^4 \sum_{i,j=1..6} \{q_{AE}\}_{ij} b_1^{2(i-1)} b_2^{2(j-1)} \right] / \left[3(b_1 b_2 + b_1 + b_2)^3 (b_1 b_2 - b_1 - b_2)^3 (b_1 b_2 + b_1 - b_2)^{\frac{7}{2}} \times (b_1 b_2 + b_2 - b_1)^{\frac{7}{2}} (b_1^2 b_2^2 - 2b_1 b_2 - b_1^2 - b_2^2) \right], \quad (28)$$

$$f_{BK} = \left[\pi^2 b_1^{10} b_2^{10} \sum_{i,j=1..14} \{q_{BK}\}_{ij} b_1^{2(i-1)} b_2^{2(j-1)} \right] / \left[5040(b_1 b_2 + b_1 + b_2)^9 (b_1 b_2 - b_1 - b_2)^9 (b_1 b_2 + b_1 - b_2)^{\frac{19}{2}} \times (b_1 b_2 + b_2 - b_1)^{\frac{19}{2}} \right], \quad (29)$$

$$f_{BE} = - \left[\pi^2 b_1^{10} b_2^{10} \sum_{i,j=1..15} \{q_{BE}\}_{ij} b_1^{2(i-1)} b_2^{2(j-1)} \right] / \left[5040(b_1 b_2 + b_1 + b_2)^9 (b_1 b_2 - b_1 - b_2)^9 (b_1 b_2 + b_1 - b_2)^{\frac{19}{2}} \times (b_1 b_2 + b_2 - b_1)^{\frac{19}{2}} (b_1^2 b_2^2 - 2b_1 b_2 - b_1^2 - b_2^2) \right], \quad (30)$$

where

$$\{q_{AK}\} = \begin{bmatrix} 0 & 0 & 0 & 0 & 3 \\ 0 & 0 & 0 & -12 & 36 \\ 0 & 0 & 18 & -36 & -55 \\ 0 & -12 & -36 & 158 & -10 \\ 3 & 36 & -55 & -10 & 26 \end{bmatrix},$$

$$\{q_{AE}\} = \begin{bmatrix} 0 & 0 & 0 & 0 & 0 & -6 \\ 0 & 0 & 0 & 0 & 18 & -39 \\ 0 & 0 & 0 & -12 & -132 & 128 \\ 0 & 0 & -12 & 342 & -224 & -90 \\ 0 & 18 & -132 & -224 & 356 & -18 \\ -6 & -39 & 128 & -90 & -18 & 25 \end{bmatrix}.$$

Matrixes $\{q_{BK}\}$ and $\{q_{BE}\}$ are given in Table III and IV respectively.

E. Potential and force between equivalent tubes

The potential and force can be expressed essentially simpler in the case when radii of interacted tubes are

TABLE I: Matrix $\{p_{BK}\}$

0	0	0	0	0	0	0	0	0	0	0	0	-19530
0	0	0	0	0	0	0	0	0	0	14490	-104685	
0	0	0	0	0	0	0	0	445410	-2015790	765744		
0	0	0	0	0	0	0	-1760850	7748055	-2248848	-1029636		
0	0	0	0	0	2758140	-938280	-36368640	27011520	-1356976			
0	-1437660	-31109610	114941568	-34271280	-35205136	5012854						
52840620	-77089824	-172119744	193452624	-11269956	-5001276							
360818280	-161478032	-132247830	47389620	1327256								
295052744	-50123640	-24636352	1062586									
Symmetry			54162000	-2009850	-786849							
				2858226	112076							
					18436							

TABLE II: Matrix $\{p_{BE}\}$

0	0	0	0	0	0	0	0	0	0	0	177345
0	0	0	0	0	0	0	0	0	0	976500	605220
0	0	0	0	0	0	0	0	-9019710	28878780	-7265496	
0	0	0	0	0	0	18117540	-26421780	-43621536	16744920		
0	0	0	0	0	4242735	-322255500	735299208	-256914792	-3437690		
0	0	-66510360	827431080	-863979648	-1027666080	746908112	-43635920				
104031900	-508237800	-2282192304	5778243552	-1895641688	-527458544	77409220					
4923519552	-4510407600	-4710377296	4534092720	-365372760	-54614168						
12018698404	-4283796976	-2131197060	690518216	8213905							
5458820144	-809953328	-276097028	11278540								
Symmetry			660421350	-23545932	-6367700						
				24951224	777760						
					114064						

TABLE III: Matrix $\{q_{BK}\}$

0	0	0	0	0	0	0	0	0	0	15624
0	0	0	0	0	0	0	0	0	-42840	755433
0	0	0	0	0	0	0	-317520	4651668	-1248828	
0	0	0	0	0	0	2109744	-40861422	65362332	-11592924	
0	0	0	0	0	-5380200	79474500	10951500	-192184440	44486040	
0	0	6971832	28477575	-991483500	1506696660	-240160680	-50195242			
0	-3356640	-318885336	2273850600	-1148679840	-2776597920	1286509520	-21785104			
492775164	-1357432104	-5600776440	10812253920	-1915609240	-1300087984	107776844				
10893073968	-7839981360	-9567436112	7173492336	-138383496	-103517008					
20757703300	-6144532400	-3892023180	951956720	33353705						
8420997520	-1012896160	-459154660	9346988							
Symmetry			973066230	-17001900	-8899384					
				37187456	1348304					
					155552					

TABLE IV: Matrix $\{q_{BE}\}$

0	0	0	0	0	0	0	0	0	0	-35469
0	0	0	0	0	0	0	0	0	-124362	-1553454
0	0	0	0	0	0	0	0	2159073	-24489990	4928091
0	0	0	0	0	0	-7426692	104520780	-139540884	17567676	
0	0	0	0	0	8202411	84564396	-901760874	861398916	-110403234	
0	0	0	0	11375658	-1024742250	4609741500	-3041479980	-594533340	204320812	
0	0	-48259071	1921604958	-3163636875	-12201112980	16321695750	-3128825524	-103004658		
68216904	-1059904440	-11093841192	45974714520	-25761560400	-14217370384	6921793360	-196048368			
21368220468	-31611088152	-55358109540	87874942896	-17650761720	-4488366288	380618007				
131005821528	-71790032408	-50711821008	34135947792	-1350545098	-270248958					
128236620500	-32263986000	-13793389735	3110622970	63736407						
33152425140	-3602984700	-1197711564	24929412							
Symmetry			2709914346	-49166500	-17323848					
				77206912	2281392					
					236192					

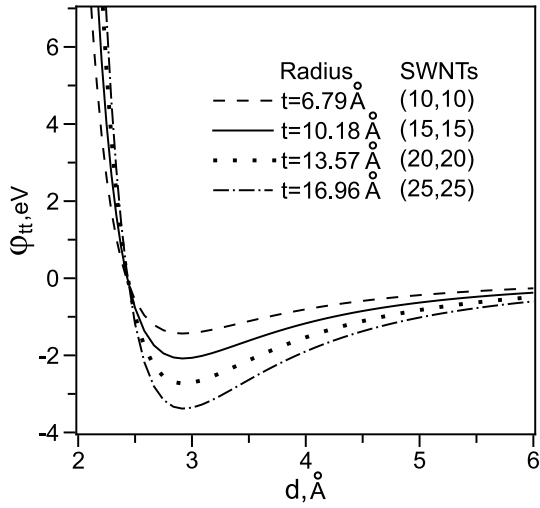


FIG. 2: Potential energies for interaction between pairs of identical SWNTs

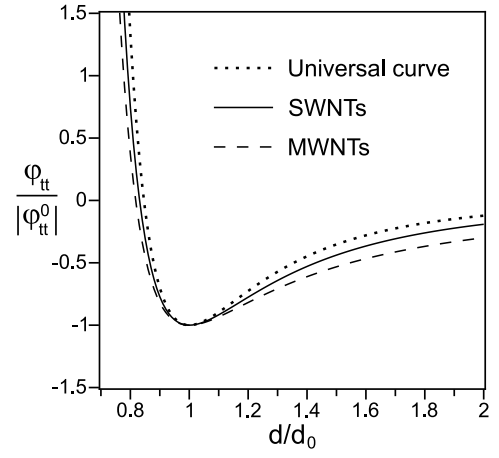


FIG. 4: Uniform potential for CNTs with arbitrary sizes. Dotted line is the universal curve suggested by L.A. Girifalco et al.

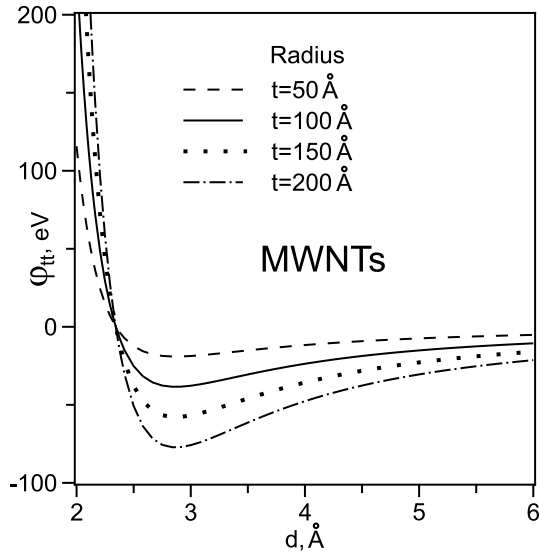


FIG. 3: Potential energies for interaction between pairs of MWNTs of equivalent size. MWNTs contain exactly 10 layers

equal $t_1 = t_2 = t$, therefore $b_1 = b_2 = b = r/t$. Then we have for potential

$$\varphi_{tt}^*(r, t) = \frac{\nu^2}{\sin \gamma} \left(-\frac{A \cdot g_A^*}{r^2} + \frac{B \cdot g_B^*}{r^8} \right), \quad (31)$$

where

$$g_A^* = g_{AK}^* K(2/b) + g_{AE}^* E(2/b), \quad (32)$$

$$g_B^* = g_{BK}^* K(2/b) + g_{BE}^* E(2/b), \quad (33)$$

and

$$g_{AK}^* = -\frac{2\pi^2(5b^2 - 4)}{3(b^2 - 4)^2}, \quad (34)$$

$$g_{AE}^* = \frac{2\pi^2(32 - 20b^2 + 11b^4)}{3(b^2 - 4)^3}, \quad (35)$$

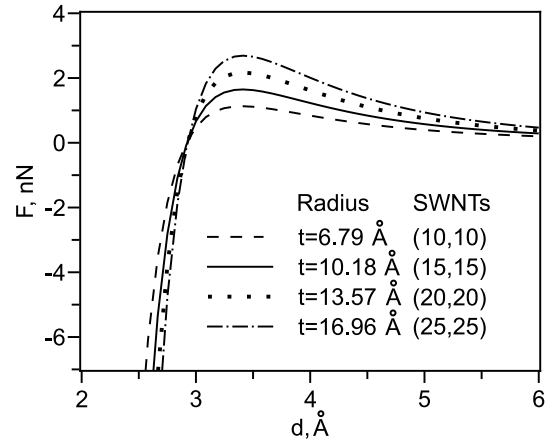


FIG. 5: van der Waals forces between two identical SWNTs

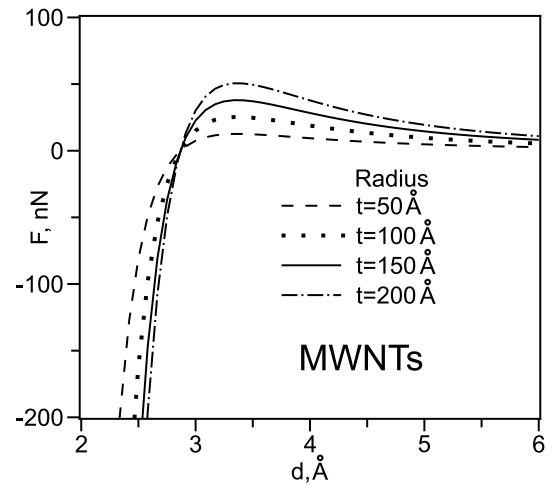


FIG. 6: van der Waals force between pairs of MWNTs of equivalent size. MWNTs contain 10 layers

TABLE V: Dependence of potential well $|\varphi_{tt}^0|$ (eV) from number of layers for MWNTs of equivalent radii

Radius (Å)	5	10	15	20	25
50	18.57	19.05	N/A	N/A	N/A
100	37.31	38.46	38.84	39.00	39.08
150	56.06	57.85	58.48	58.78	58.95
200	74.81	77.25	78.11	78.54	78.79

$$g_{BK}^* = -\pi^2(4609b^{14} + 56038b^{12} + 321132b^{10} - 473632b^8 + 1885952b^6 - 3867648b^4 + 4510720b^2 - 2293760)/(1575(b^2 - 4)^8), \quad (36)$$

$$g_{BE}^* = \pi^2(7129b^{16} + 97220b^{14} + 763489b^{12} - 1533424b^{10} + 7790944b^8 - 21756160b^6 + 38781184b^4 - 40099840b^2 + 18350080)/(1575(b^2 - 4)^9). \quad (37)$$

By totally the same way in the case of $t_1 = t_2$ for force we have

$$F^*(t, r) = \frac{\nu^2}{\sin \gamma} \left(-\frac{Af_A^*}{t^2} + \frac{Bf_B^*}{t^8} \right), \quad (38)$$

$$f_A^* = \frac{4\pi^2}{3b^3(b^2 - 4)^4} \left(f_{AK}^* K\left(\frac{2}{b}\right) + f_{AE}^* E\left(\frac{2}{b}\right) \right), \quad (39)$$

$$f_B^* = \frac{\pi^2}{315b^9(b^2 - 4)^{10}} \left(f_{BK}^* K\left(\frac{2}{b}\right) + f_{BE}^* E\left(\frac{2}{b}\right) \right), \quad (40)$$

$$f_{AK}^* = 13b^6 - 62b^4 + 64b^2 - 96, \quad (41)$$

$$f_{AE}^* = -25b^6 + 36b^4 - 176b^2 + 192, \quad (42)$$

$$f_{BK}^* = 9722b^{18} + 129650b^{16} + 537641b^{14} - 5804036b^{12} + 11418976b^{10} - 50923136b^8 + 118211840b^6 - 180548608b^4 + 162971648b^2 - 66060288, \quad (43)$$

$$f_{BE}^* = -14762b^{18} - 285174b^{16} - 2659951b^{14} + 3029636b^{12} - 27622752b^{10} + 95326336b^8 - 226611968b^6 + 351556608b^4 - 321814528b^2 + 132120576. \quad (44)$$

III. RESULTS AND DISCUSSION

We have studied the WDV interaction between two crossed CNTs by using the continuum LJ approximation. The analytical integrations for the potential energy of interaction between two identical SWNTs are plotted in Fig. 2. We assume nanotubes are crossed at a right angle in all our following illustrations and calculations both for SWNTs and MWNTs. We use parameter $d = r - 2t$ to characterize the distance between tubes. Based on the results illustrated in Fig. 2, it can be concluded that real gap between surfaces of interacting SWNTs in equilibrium state is changed slightly in range $d = 2.92..2.93$ Å. This distance is practically independent from the angle of nanotube intersection and the diameter proportion. For comparison in Ref. 21 the equilibrium gap between two fullerenes C_{60} is given as 2.95 Å.

In the case of MWNTs interaction we apply another attractive ($A = 18.6\text{eV} \cdot \text{Å}^6$) and repulsive ($B = 29040\text{eV} \cdot \text{Å}^{12}$) constants which reproduce the layer distance of 3.35 Å and the elastic constant $C_{33} = 4.08$ GPa of graphite³⁷. We assume that each pair of layers interacts as SWNTs and use summation over all pairs. The potential energy for two MWNTs of equivalent radii is plotted in Fig. 3. In these calculations we assume that each MWNT consists exactly of 10 walls. The equilibrium distance between their surfaces is found to be $d_0 = 2.87$ Å, which is smaller than the equilibrium SWNT-SWNT gap. From our calculations follows that only several outer shells of MWNTs play essential role in the VDW interaction. For example, if two equal MWNTs with $d = 200$ Å contain 5, 10, 15, 20 or 25 layers then the minimum energy is -74.8, -77.2, -78.1, -78.5 or -78.8 eV respectively. Dependence of the minimum potential energy from number of inner layers for pairs of equivalent MWNTs is presented in Table V.

It was found that the VDW interaction between $C_{60} - C_{60}$, C_{60} -SWNT, C_{60} -graphene, graphene-graphene, parallel SWNT-SWNT, and parallel MWNT-MWNT can be described by a universal curve^{29,34,40}. In our case universal curve means that a plot of $\bar{\varphi}_{tt} = \varphi_{tt}^0/|\varphi_{tt}^0|$ against $\bar{d} = d/d_0$ gives the same curve for all tube-tube interactions, where φ_{tt}^0 is the minimum energy and d_0 is the equilibrium spacing for the two crossed tubes. As pointed above, the equilibrium distances are approximately constants both for SWNTs and MWNTs.

We have calculated the minimum energy φ_{tt}^0 for SWNTs of different radii (Table VI) as well as for MWNTs (Table VII). These results can be described by approximating formula

$$\varphi_{tt}^0 = C_1^{CNT} \sqrt{t_1 t_2} + C_2^{CNT} \frac{t_1 + t_2}{\sqrt{t_1 t_2}},$$

where $C_1^{SWNT} = -0.19285\text{eV} \cdot \text{Å}^{-1}$, $C_2^{SWNT} = -0.05847\text{eV}$, and $C_1^{MWNT} = -0.388\text{eV} \cdot \text{Å}^{-1}$, $C_2^{MWNT} = 0.186\text{eV}$ are parameters for SWNTs and MWNTs respectively. It can be figured out from Tables VI and VII that

TABLE VI: Calculated depth $|\varphi_{tt}^0|$ (eV) for SWNTs (upper-right side) and approximation (lower-left side)

Tube type	(10,10)	(15,15)	(20,20)	(25,25)	
Radius (\AA)	6.79	10.18	13.57	16.96	
(10,10)	6.79	1.426 \ 1.434	1.728	1.979	2.202
(15,15)	10.18	1.723	2.080 \ 2.081	2.384	2.653
(20,20)	13.57	1.975	2.385	2.734 \ 2.731	3.039
(25,25)	16.96	2.199	2.655	3.043	3.388 \ 3.382

TABLE VII: Calculated depth $|\varphi_{tt}^0|$ (eV) for MWNTs consisting of 10 shells (upper-right side) and approximation (lower-left side)

Radius (\AA)	50	100	150	200
50	19.03 \ 19.05	27.07	33.20	38.36
100	27.04	38.43 \ 38.46	47.17	54.51
150	33.17	47.14	57.83 \ 57.85	66.85
200	38.33	54.48	66.83	77.23 \ 77.25

approximating formula gives very good accuracy. Using dimensionless potential $\overline{\varphi}_{tt}$ we can fit the potential of interaction between pairs of different SWNTs to one uniform curve and between pairs of different MWNTs to another one (Fig. 4).

It is remarkable that plots for CNTs of the different radii fall down in the corresponding curves with accuracy of line thickness. For comparison Fig. 4 also shows a universal potential suggested by Girifalco L.A. et al.²⁹.

Figs. 5 and 6 show forces for two CNTs of equivalent radii. As we see in figures the behavior both for SWNTs and for MWNTs is qualitatively similar. The distance where attractive force reaches its maximum is in range 3.40-3.41 for SWNTs and it is practically constant, 3.36 \AA for MWNTs.

IV. SUMMARY AND CONCLUSIONS

In summary, we used Lennard-Jones potential for two carbon atoms and apply method of the smeared out ap-

proximation suggested by L.A. Girifalco to calculate interaction between two crossed CNTs of uniform and different diameters. The exact formulas for potential energy and van der Waals forces are expressed in terms of rational and elliptical functions. These formulas become essentially simpler in the case of interaction between equivalent tubes. We estimated the equilibrium distance, maximal attractive force and potential energy for SWNTs and MWNTs. We plotted uniform potential for SWNTs and MWNTs.

V. ACKNOWLEDGMENTS

We gratefully acknowledge support through the National Science Council of Taiwan, Republic of China, through the project NSC 95-2112-M-001-068-MY3.

* Electronic address: evgeny@gate.sinica.edu.tw

¹ M. P. Anantram and F. Léonard, Rep. Prog. Phys. **69**, 507 (2006).

² A. I. Zhbanov, N. I. Sinitsyn, and G. V. Torgashov, Radiophysics and Quantum Electronics **47**, 435 (2004).

³ P. Kim and C. M. Lieber, Science **286**, 2148 (1999).

⁴ C.-H. Ke, N. Pugno, B. Peng, and H. D. Espinosa, Journal of the Mechanics and Physics of solids **53**, 1314 (2005).

⁵ M. Dequesnes, S. V. Rotkin, and N. R. Aluru, Nanotechnology **13**, 120 (2002).

⁶ J. M. Kinaret, T. Nord, and S. Viefers, Applied Physics Letters **82**, 1287 (2003).

⁷ A. Ramezani, A. Alasty, and J. Akbari, International Journal of Solids and Structures **44**, 4925 (2007).

⁸ J. Cumings and A. Zettl, Science **289**, 602 (2000).

⁹ L. Dong, F. Arai, and T. Fukuda, IEEE Transactions on Mechatronics **9**, 350 (2004).

¹⁰ L. Dong, B. J. Nelson, T. Fukuda, and F. Arai, IEEE Transactions on Automation Science and Engineering **3**, 228 (2006).

¹¹ T. Rueckes, K. Kim, E. Joselevich, G. Y. Tseng, C.-L. Cheung, and C. M. Lieber, Science **289**, 94 (2000).

¹² O.-K. Kwon, J. W. Kang, K. R. Byun, J. H. Lee, and H. J. Hwang, NSTI-Nanotech **2**, 234 (2005).

- ¹³ J. E. K. Doye and D. J. Wales, *Chemical Physics Letters* **247**, 339 (1995).
- ¹⁴ S. B. Sinnott, R. Andrews, D. Qian, A. M. Rao, Z. Mao, E. C. Dickey, and F. Derbyshire, *Chemical Physics Letters* **315**, 25 (1999).
- ¹⁵ J. I. Sohn and S. Lee, *Appl. Phys. A* **74**, 287 (2002).
- ¹⁶ J. Tersoff and R. S. Ruoff, *Phys. Rev. Lett.* **73**, 676 (1994).
- ¹⁷ L. Henrard, E. Hernández, P. Bernier, and A. Rubio, *Physical Review B* **60**, R8521 (1999).
- ¹⁸ J.-L. Sauvajol, E. Anglaret, S. Rols, and L. Alvarez, *Carbon* **40**, 1697 (2002).
- ¹⁹ L. A. Girifalco and R. A. Lad, *Journal of Chemical Physics* **25**, 693 (1956).
- ²⁰ W. Allers, A. Schwarz, U. D. Schwarz, and R. Wiesendanger, *Applied Surface Science* **140**, 247 (1999).
- ²¹ L. A. Girifalco, *Journal of Physical Chemistry* **96**, 858 (1992).
- ²² K. Kniaż, L. A. Girifalco, and J. E. Fischer, *J. Phys. Chem.* **99**, 16804 (1995).
- ²³ H. Guérin, *J. Phys.: Condens. Matter* **10**, L527 (1998).
- ²⁴ D. Baowan, N. Thamwattana, and J. M. Hill, *Eur. Phys. J. D* **44**, 117 (2007).
- ²⁵ C. Rey, J. García-Rodeja, L. J. Gallego, and J. A. Alonso, *Phys. Rev. B* **55**, 7190 (1997).
- ²⁶ S. Guo, P. M. Nagel, A. L. Deering, S. M. Van Lue, and S. A. Kandel, *Surface Science* **601**, 994 (2007).
- ²⁷ N. D. Drummond and R. J. Needs, *Physical Review Letters* **99**, 166401 (2007).
- ²⁸ S. J. Sque, R. Jones, S. Oberg, and P. R. Briddon, *Physical Review B* **75**, 115328 (2007).
- ²⁹ L. A. Girifalco, M. Hodak, and R. S. Lee, *Phys. Rev. B* **62**, 13104 (2000).
- ³⁰ W. Mickelson, S. Aloni, W.-Q. Han, J. Cumings, and A. Zettl, *Science* **300**, 467 (2003).
- ³¹ D. Baowan, N. Thamwattana, and J. M. Hill, *Physical Review B* **76**, 155411 (2007).
- ³² B. J. Cox, N. Thamwattana, and J. M. Hill, *Current Applied Physics* **8**, 249 (2008).
- ³³ N. Thamwattana and J. M. Hill, *J. Nanopart. Res.* **10**, 665 (2008).
- ³⁴ C.-H. Sun, L.-C. Yin, F. Li, G.-Q. Lu, and H.-M. Cheng, *Chemical Physics Letters* **403**, 343 (2005).
- ³⁵ D. Cao and W. Wang, *Chemical Engineering Science* **62**, 6879 (2007).
- ³⁶ A. Popescu, L. M. Woods, and I. V. Bondarev, *Physical Review B* **77**, 115443 (2008).
- ³⁷ R. Saito, R. Matsuo, T. Kimura, G. Dresselhaus, and M. S. Dresselhaus, *Chemical Physics Letters* **348**, 187 (2001).
- ³⁸ D. Baowan and J. M. Hill, *Z. angew. Math. Phys.* **2007**, 857 (2007).
- ³⁹ T. Xiao and K. Liao, *Composites: Part B* **35**, 211 (2004).
- ⁴⁰ C.-H. Sun, G.-O. Lu, and H.-M. Cheng, *Physical Review B* **73**, 195414 (2006).
- ⁴¹ Q. Zheng, J. Z. Liu, and Q. Jiang, *Physical Review B* **65**, 245409 (2002).
- ⁴² M. Abramowitz and I. A. Stegun, *Handbook of mathematical functions* (Dover Publications, New York, 1964), chap. 17.
- ⁴³ H. Hancock, *Lectures on the theory of Elliptic functions* (J. Wiley & Sons, New York, 1910).
- ⁴⁴ A. G. Greenhill, *The applications of elliptic functions* (Macmillan, New York, 1892).
- ⁴⁵ L. V. King, *On the direct numerical calculation of Elliptic functions and integrals* (Cambridge University Press, 1924).